On the parameterization of single pole adaptive notch filter against wide range of linear chirp interference

Syed Ali Kazim, Juliette Marais, Nourdine Aït Tmazirte

On the parameterization of single pole adaptive notch filter against wide range of linear chirp interference

Syed Ali Kazim*, Juliette Marais*, Nourdine Aït Tmazirte *.

* COSYS-LEOST, Univ Gustave Eiffel, Univ Lille,
F-59650 Villeneuve d'Ascq, FRANCE
email: {syed-ali.kazim, juliette.marais,
nourdine.ait-tmazirte}@univ-eiffel.fr

Biographies

Syed Ali Kazim has a master's degree in Electronic Engineering. He received a specialization degree in Navigation and Related Applications from Politecnico di Torino (Italy) in 2017. He is currently a Ph.D. student at University Gustave Eiffel. His research activities are mainly devoted to GNSS signal characterization, error modeling, filtering techniques and localization systems.

Nourdine Aït Tmazirte is a research engineer at University Gustave Eiffel since 2021. He got his engineering and M.Sc. degree in automation engineering from Ecole Centrale de Lille, France, both in 2010. His research interests include multi-sensor fault-tolerant fusion for localization and integrity assessment.

Dr. Juliette Marais received an engineering degree from Institut Supérieur de l'Electronique et du Numérique. She received a Ph.D. degree in electronics and the "Habilitation à diriger des recherches" from the University of Lille, France, in 2002 and 2017 respectively. Since 2002, she has been a research fellow with Université Gustave Eiffel (former IFSTTAR). She is involved in projects aiming the development of fail-safe uses of GNSS-bases solutions in land transport applications with contributions in EU or national projects. Her research interests principally include propagation phenomena, positioning and pseudorange error modeling, filtering technics, integrity concepts and simulation.

Abstract

Radio frequency interferences (RFIs) poses a severe threat to Global Navigation Satellite System (GNSS). It is one of the main concerns that continue to challenge GNSS deployment in safety-related applications. Adaptive Notch Filter (ANF) is a classical method often used for the suppression of chirp signals. However, ANF performance is conditioned to the parameters selection where an inappropriate choice could also have a negative consequence. The adaptation step and pole contraction factor are mostly the two important parameters controlling the filter dynamics and suppression level. An appropriate compromise is needed while keeping in view the characteristics of the chirp signal. This study proposes a parameterization approach for ANF while dealing with a wide range of chirp signals with different values of sweep bandwidth, sweep rate, and power level. To provide labels RMSE criterion is investigated at the signal level before the de-spreading process. Finally, a generalized multivariate polynomial regression (MPR) model is presented that takes sweep bandwidth, sweep rate and power level as input features and predicts the values of pole contraction factor and adaptation step. To validate the performance of ANF with the predictions, three scenarios with different chirp signals exhibiting slow, moderate and fast variations are presented. The mitigation performance is analyzed in several levels including, interference frequency estimation, satellite signal tracking, carrier-to-noise ratio and most importantly on positioning KPIs such as accuracy, availability and safety.

Introduction

Satellite positioning systems are undeniably an asset in the catalog of positioning solutions for transport systems. In contrast to any other positioning systems, they provide an inexpensive solution for the users to geographically localize without any a priori information. However, when it comes to the development of localization functions for land transportation systems, positioning reliability becomes a key paramount for safety-critical applications. Indeed, GNSS is still very often (and sometimes hastily) considered an unreliable system due to intrinsic vulnerabilities. This includes the problem of satellite masking, multipath and intentional or unintentional radio frequency interference. The literature over the last two decades has considerably developed methodologies to tackle multipath and NLOS phenomena. Concerning radio frequency interference, the nature of the threat could vary so as the impact with change in the signal characteristics. Interference countermeasures could be possibly applied at different levels of the receiver processing chain including the Front end, pre-correlation, post correlation and navigation level (Dovis, 2015). These techniques can be generally grouped based on the resource requirements: 1) signal processing methods (Anyaegbu et al., 2008; Borio, 2016; Borio et al., 2008; Borio & Cano, 2013; Dovis et al., 2012) applied directly to the recorded signal in the time domain or transformation domain by projecting the time series signal to either frequency, time-frequency or time-scale domain; 2) Spatial filtering (Fu et al., 2003; Gupta & Moore, 2003; Stallo et al., 2020) requires additional antennas to acquire signals coming from multiple directions with different delays due to antennas arrangement. This allows to control numerically the antenna gain by steering it in the direction of the satellite signals while suppressing the signal coming from the direction of the interference source; 3) Vector tracking (Dey et al., 2021) takes advantage of satellite channels redundancy to enhance the overall performance by cooperating in the tracking process; 4) sensor fusion (Groves & Long, 2005) uses additional measurements coming from inertial sensors to improve the performance of the multi-sensor localization system in the presence of interference.

This study addresses the limitation of ANF found in the previous work (Kazim, Marais, et al., 2022) where we presented a comparative analysis of interference mitigation using an adaptive notch filter and wavelet packet decomposition method against frequency hopping and linear chirp signals. In the case of linear chirp, the two methods (WPD and ANF) showed highly comparable results regardless of the weighting model used to estimate the position. The mitigation strategies significantly improved position accuracy but led to a non-negligible amount of unavailability. These observations lead us to a hypothesis that optimally tuned ANF could further improve the performance to an acceptable level, which could be only possible by finding a necessary compromise between the convergence time and tracking oscillations. (Qin et al., 2019) previously discussed the significance of the appropriate parameter choice in suppressing the chirp signal. Also, inappropriately chosen parameters not only affects the removal of interference but could also induce severe distortions in the useful content. However, there is no manner to generalize the tunable parameter for chirp signals with different characteristics. This study deals with the ANF parametrization for a wide range of chirp signals with different bandwidths, sweep rates and power levels. A multivariate polynomial regression (MPR) approach is presented to model the tunable parameters. The complete process involves several steps: 1) creation of the database containing wide range of chirp signals with different bandwidth, sweep rate and power levels. Each interference scenario is added while replaying the GNSS reference IQs using playback system. The interference signals are recorded and the files are added to the database, 2) labelization process requires giving tagging all the scenarios in the database with optimal ANF configuration. A root mean square error (RMSE) criterion is adopted comparing the average error between the reference signal and the filtered signal. Several ANF configurations with different values of pole factor and adaptation step are tested and only one combination with minimum RMSE value is selected per scenario. 3) Regression and Generalization. The regression is done in 2 steps. In the first step, a third-order multivariate regression is performed considering only 2 features (bandwidth and sweep rate). In the second step, a third-order mono-variable polynomial regression is performed on each MPR coefficient to generalize the effects of the power level. 4) Prediction. Finally, the generalized multivariate polynomial regression (GMPR) model is used to predict the values of the adaptation step and pole contraction factor for three scenarios with low, moderate and fast varying chirp with different power levels.

The paper is structured as follows: Section 1 brefly introduces some fundamentals on interference, potential systems that could interfere with the GNSS band, their spectral characteristics particularly the intentional interference form the personal privacy devices transmitting chirp-like signal, also describe in detail the mitigation

method based on adaptive notch filter and the role of tuning parameters in the convergence and the traking noise. The section 2 provides the proposed modeling approach to obtain optimal parameters for the ANF with all the processes involved in the modeling including database creation, labelization with optimal parameter combination (adaptation step and the pole contraction factor) after exausively applying ANF while changing the parameters, a 2-step generalized multivariate polynomial regression (MPR) models for each input parameter taking into account the 3 feature of linear chirp (bandwidth, sweep rate and the power level) and the predictions for the test scenarios. The section 3 provides a detailed comparative discussion on the ANF mitigation performance in interference frequency estimation, satellite tracking, carrier to noise ratio and positioning KPIs (accuracy, availabity, safety), using the predicted values from the models and naively chosen combination, conclusions and perspectives to close the discussion.

I. Interferences: Sources & Suppression Techniques at Precorrelation Level

The satellite signals arriving at the receiver antenna are very weak due to a large propagation distance between the satellites and the receiver placed on the ground. This intrinsic weakness of GNSS signals makes them vulnerable to any communication systems transmitting signals within the same band or even close to the band of interest. The presence of an interference signal can severely degrade the performance of the receiver even possibly it could completely block the signals depending on the severity of the signal generated from the interfering source.

A. Interference sources and signal characteristics

Radio Frequency Interferences (RFI) can be of different forms and can be grouped broadly into two main streams based on the purpose of intent. It could be either generated intentionally with a deliberate target or unintentionally by other communication systems. Indeed, the frequency bands allocated to GNSS signals are internationally protected but, despite the regulations, the use of personal privacy devices (PPDs) is very common and the pervasive use of wireless systems has also increased the interference issues. Table 1 provides some common interference sources and the type of interfering signals.

Table 1. Types of interference signals with some typical sources.

Types of interference	Some typical sources
Wideband Gaussian	Intentional noise jammer
Wideband phase/frequency modulation	Television broadcast (harmonics)
Wideband spread spectrum	Intentional spread spectrum jammer
Wideband pulse	Radar transmitters
Narrowband phase/frequency modulation	AM station and CB transmitter (harmonics)
Narrowband-swept continuous wave	FM station (harmonics) and intentional CW jammer
Narrowband continuous wave	Intentional CW jammers and near-band unmodulated carrier frequency

The interfering signal generated from various sources can come in many different forms. However, every interfering signal has a specific footprint describing the characteristics of the signal. Figure 1 illustrates the spectral features of some very common interference signals including monotone Amplitude Modulation (AM), Frequency hopping, Chirp and DME-like signals.

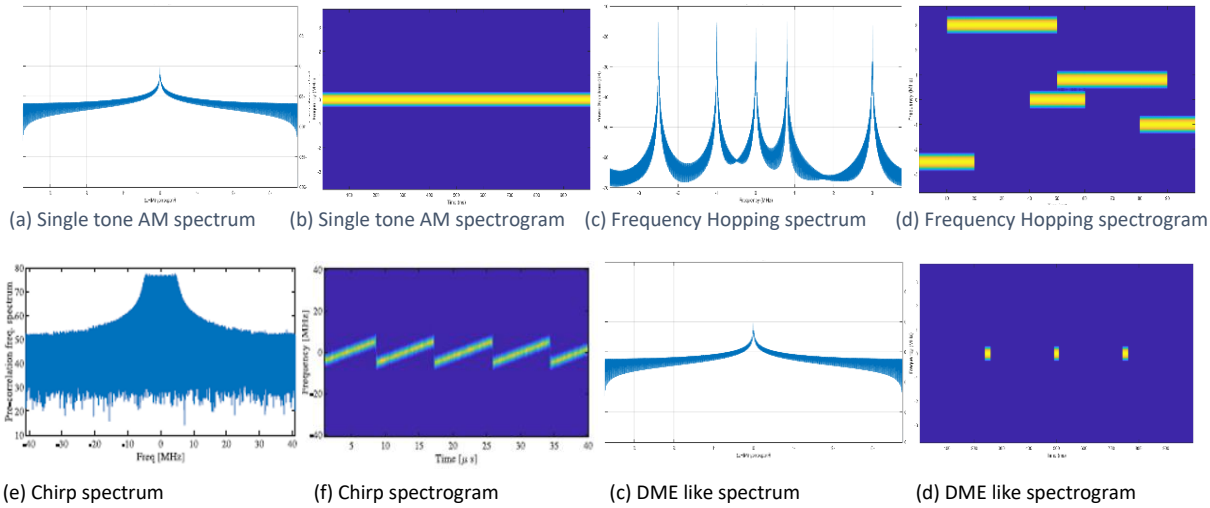

(a) Single tone AM spectrum (b) Single tone AM spectrogram (c) Frequency Hopping spectrum (d) Frequency Hopping spectrogram

(e) Chirp spectrum (f) Chirp spectrogram (c) DME like spectrum (d) DME like spectrogram

Figure 1. The spectral characteristics of some typical interference signals in the baseband

According to (Kraus et al., 2011), the linear chirp belongs to the category II jammer because of the difficulty level in the detection and it is mainly characterized by the sweep direction, bandwidth, sweep rate and the power. The linear chirp is a periodic frequnecy modulated signal in which the instantenous frequency of the signal linearly changes over the time in each period. The mathematical model of the chirp signal is given as:

$$x(t)_{chirp} = \sqrt{P_J}\, e^{(j\,(f_q(t)t + \theta_J)}$$

where P_J is the power, θ_J is the initial phase, t is the time instance and $f_q(t)$ is the instantenous frequency of the jamming signal over the period of time. The instantenous frequency is written as:

$$f_q(t) = 2\pi f_J t + \pi b \frac{(f_{max} - f_{min})}{T_{sweep}}\, t^2$$

Where f_J is the starting frequency, b is the sweeping direction which can be either in the up direction ($b = +1$) or down direction ($b = -1$), T_{sweep} is the sweep period and $f_{min} - f_{max}$ is the sweep bandwidth with f_{min} and f_{max} is the minimum and the maximum frequency respectively.

B. PRE-CORRELATION LEVEL MITIGATION TECHNIQUE: ADAPTIVE NOTCH FILTER

Among the different families of mitigation techniques addressed in the introduction, let's have a look in particular to the pre-correlation-based techniques. Several signal processing approaches have been investigated for the detection and mitigation of interference. The most commonly used techniques include Pulse Blanking (PB) (Borio & Cano, 2013), Adaptive Notch Filtering (ANF) (Felber, n.d.), Short Time Fourier transform (STFT) (Borio et al., 2008), Wavelet Transform (WT) (Musumeci & Dovis, 2014) and Kerhunen-Loève Transform (KLT) (Szumski & Eissfeller, 2013).

Adaptive Notch Filter (ANF) is widely investigated and the most recommended technique to mitigate frequency modulated continuous wave (FMCW) also known as chirp signal. It is the extension of classical Notch Filter (NF) with an additional integrated adaptation unit. The purpose of an adaptation block is to continuously follow the frequency variations of the unwanted signal whereas NF applies the

Notch to remove a narrow portion of the spectrum. Several implementations of NF exist but due to implementation simplicity single-pole infinite impulse response (IIR) has gained much attention. The transfer function of a digital single pole IIR notch filter is given as:

$$\mathrm{H(z)} = \frac{1 - \hat{\mathrm{z}}_0[n]\mathrm{z}^{-1}}{1 - \mathrm{k}_\alpha \hat{\mathrm{z}}_0[n]\mathrm{z}^{-1}}$$

where k_α is the pole contraction factor that regulates the notch bandwidth and $\hat{\mathrm{z}}_0[n]$ is the filter zero that defines the position of the notch in the complex plane. The relation between notch frequency and the transfer function zero is given as:

$$z_0[n] = a_0 e^{j\,2\pi\,\hat{f}_0 T_s}$$

where $\hat{f}_0$ is the instantaneous notch frequency, a_0 is the amplitude of the complex estimate $\hat{\mathrm{z}}_0[n]$ and $T_s = 1/f_s$ is the sampling interval. The 3-dB bandwidth in terms of pole contraction factor can be estimated as:

$$B_{3dB} \approx (1 - k_\alpha) f_s\, \pi/10$$

The notch bandwidth is usually kept smaller to target a very narrow portion of the spectrum and consequently to preserve at most the useful content of the signal. The value of pole contraction must be selected in the range $k_\alpha \in [0, 1]$ for the stability of the filter. Figure 2a shows the magnitude response of $\mathrm{H}(z)$ for different values of k_α and with an amplitude $a_0 = 1$. The bandwidth of the notch gets narrower as the value of $k_\alpha \rightarrow 1$. The amplitude a_0 of the complex estimate $\hat{\mathrm{z}}_0$ determines the depth of the notch. Figure 2b shows the magnitude response of $\mathrm{H}(z)$ for different values of amplitude using a pole factor $k_\alpha = 0.9$. The notch filter acts as an all-pass filter when $a_0 = 0$ and applies spectral null when the amplitude $a_0 = 1$.

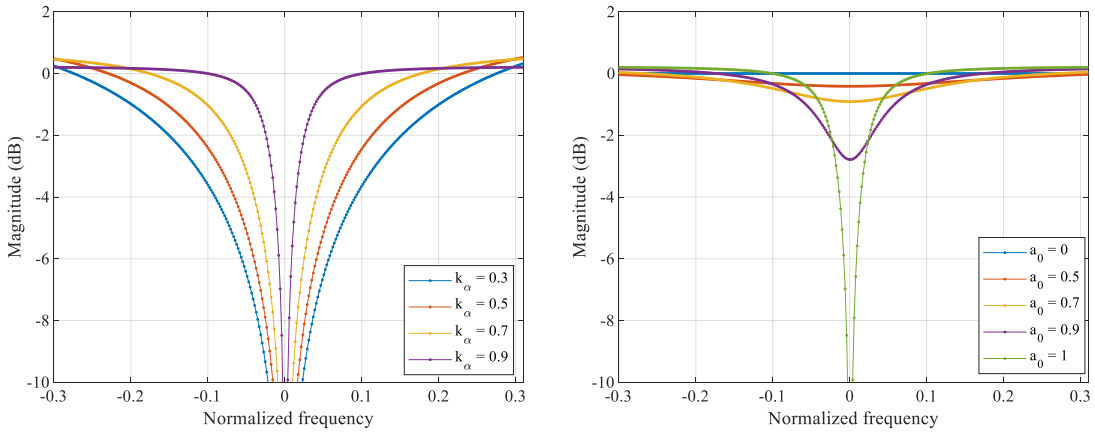

Figure 2. Magnitude response of the transfer function $H(z)$ against a) different values of pole factor (k_α) with a_0 = 1 (left) and b) different values of complex amplitude (a_0) with k_α = 0.9

The adaptation algorithm drives the notch position by moving $\hat{\mathrm{z}}_0$ in the complex plane until it converges to the interference frequency. A least mean square (LMS) based gradient descent algorithm is applied to minimize the cost function and the value of $\hat{\mathrm{z}}_0$ is estimated at each sample instance.

$$z_0[n] = z_0[n-1] - \mu[n]\, g(J[n])$$

where $g(.)$ is the stochastic gradient of the cost function $J[n]$ and $\mu[n]$ is the normalized algorithm step given as:

$$\mu[n] = \frac{\delta}{\{E|x_r[n]|^2\}}$$

where $\{E|x_r[n]|^2\}$ is the power of the autoregressive block output and δ is the adaptation step that controls the algorithm convergence.

Figure 3 shows the notch frequency estimated for different values of the adaptation step with a fixed value of the pole contraction factor $k_\alpha = 0.8$. A GPS L1 signal sampled at 15 MHz, interfered with a chirp signal with 5 MHz bandwidth, 50 µs sweep rate and 15 dB JNR. A smaller value of the adaptation step ($\delta = 0.01$) shows lower oscillations in the ramp region as the algorithm closely follows the frequency variations however during the transition it increases the convergence time. Conversely, a larger value of the adaptation step ($\delta = 0.1$) induces relatively more noise but allows quick convergence.

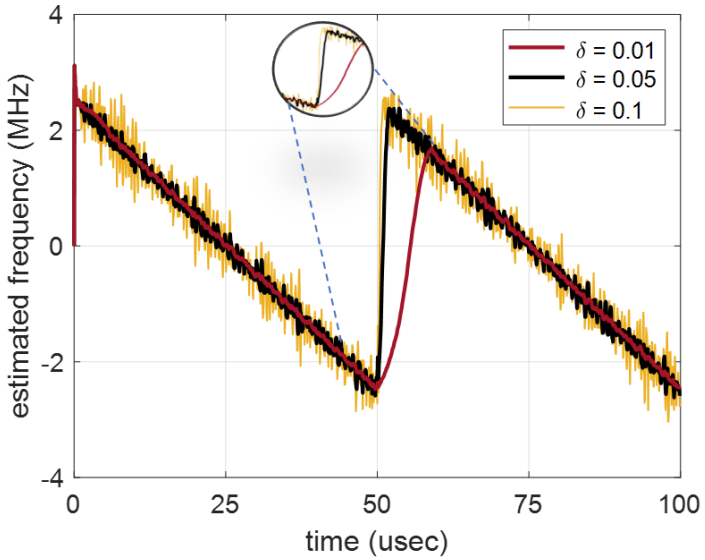

Figure 3. Interference tracking performance for different values of adaptation step (δ) with k_α = 0.8 against chirp interference (Bandwidth = 5MHz, repetition rate = 50 µs and JNR = 15 dB)

Previous work summary

The performance of the ANF-based mitigation method highly relies on the selection of previously presented parameters. An inappropriate choice not only makes this technique ineffective but can also induce severe distortions in the signal. For this reason, it demands some expertise to first understand interference signal characteristics and then for setting up the filter parameters. This would drive the filter to follow the signal dynamics, to optimally position the notch to remove the unwanted content from the signal. (Qin et al., 2020) presented several metrics in the acquisition and the tracking level to evaluate distortion induced due to interference and also from the filtering operation.

In most of the studies found in the literature, the performance of interference mitigation solutions is mainly evaluated from the signal perspective. The impact on interference frequency estimation, signal acquisition and tracking stage is then presented. (Borio & Gioia, 2021; Kazim, Tmazirte, et al., 2022)

took a further step and discussed the interference issue from the positioning perspective. The premier evaluated the impact on the positioning accuracy latter also studied the horizontal protection level (HPL) against the particular interference condition under investigation. This study finds motivation from (Kazim, Marais, et al., 2022) which provided a compressive experimental analysis on the issue of interference, analyzing the performance of two mitigation techniques on the interference frequency estimation, tracking stage, CN0, positioning accuracy, availability, and safety. The first results displayed that the interferences without any mitigation strategy have an adverse impact at each level in the presented scenario. Indeed, in the considered scenario, the interfering signal completely overpowered the satellite signal compelling the tracking loop to deviate and follow the chirp signal. This increased CN0, even higher than in the nominal conditions. This further elevated the problem from a safety point of view. HPL computation involving CN0 underestimated the protection level by giving more confidence to these measurements and bringing HMI points. We then investigated two different interference mitigation techniques; Wavelet packet decomposition (WPD) and ANF. And in particular, we applied ANF with an adaptation step $\delta = 0.05$ and a pole contraction factor $k_\alpha = 0.8$. The filtering operation considerably suppressed the interference signal by closely following the frequency variations of the chirp signal. Primarily it allowed to continue tracking the satellite signal with some additional noise due to filtering operation. From the positioning perspective, it significantly improved the positioning accuracy with no HMI. However, it compromised availability to ensure safe positioning as the integrity monitoring algorithm considered carried notably large number of epochs to be unavailable. As discussed previously, the performance of ANF is subjected to the choice of the parameters used while initializing the filter. To our knowledge, there are no existing studies that provide a manner to optimally tune ANF. For this reason, in our previous investigation, we randomly selected parameters value within the interval recommended by the literature. In this study, the motivation is to maximize ANF capabilities in suppressing the linear chirp signal. We propose an empirical method that provides optimal parameter combinations to tune ANF considering the characteristics of the interference signal.

II. PROPOSED APPROACH FOR OPTIMAL PARAMETER SELECTION

In this study, we detail an empirical approach that permits the selection of the adaptation step and pole contraction factor to initialize ANF. It takes interference signal features as the input for modeling the trend of each parameter from the measurements. These features include power, sweep rate and the sweep bandwidth that describes the characteristics of the chirp signal. The models are represented by two polynomial equations for each parameter, expressed as a function of considered input features. This approach requires rigorous and exhaustive processes involving data preparation, search of the optimal parameters and data modeling as summarized in figure 4. Each of the blocks will be described in the following.

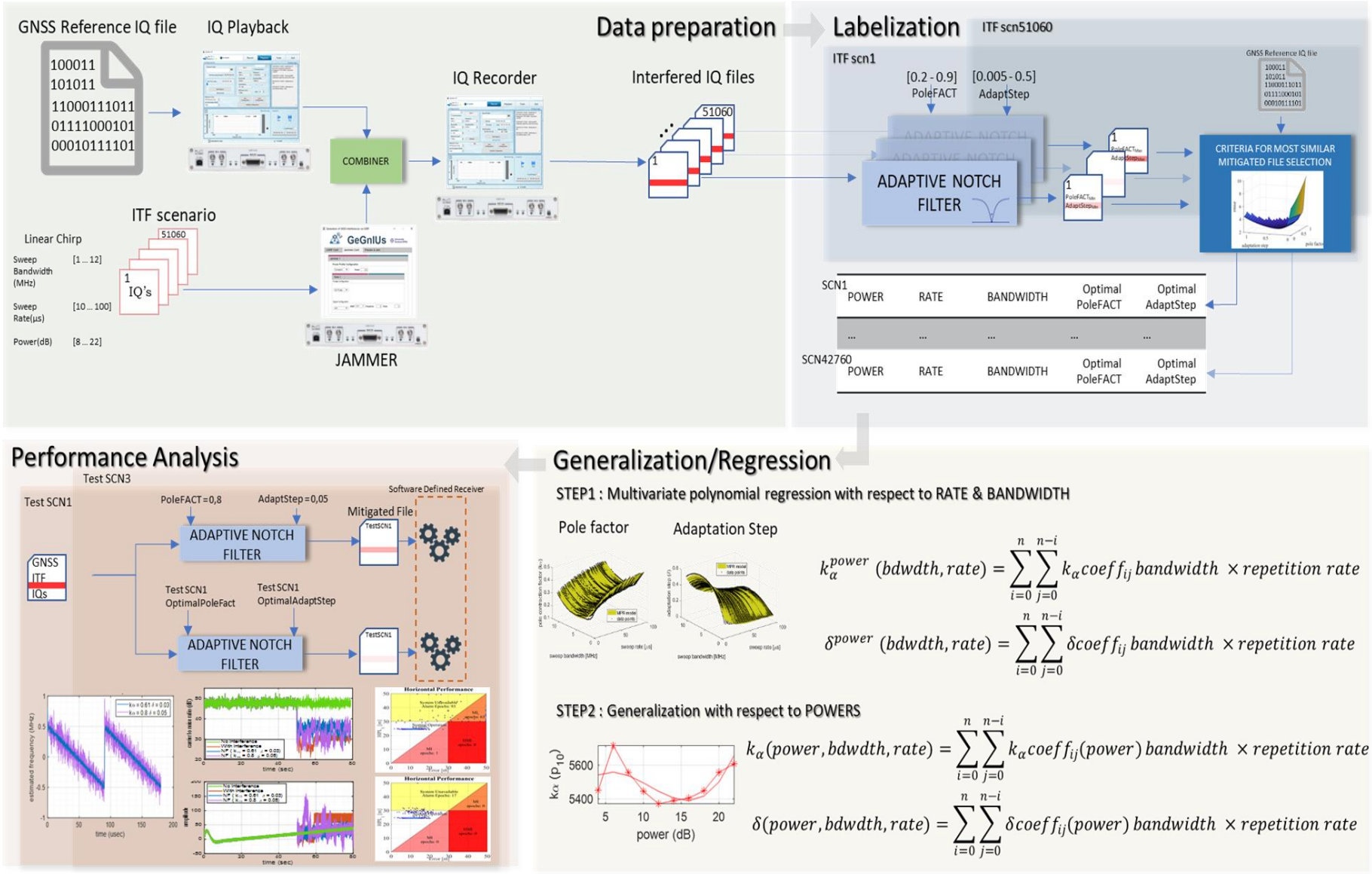

$$k_\alpha^{power}\ (bdwdth, rate) = \sum_{i=0}^{n}\sum_{j=0}^{n-i} k_\alpha coeff_{ij}\, bandwidth\ \times repetition\ rate$$

$$\delta^{power}\ (bdwdth, rate) = \sum_{i=0}^{n}\sum_{j=0}^{n-i} \delta coeff_{ij}\, bandwidth\ \times repetition\ rate$$

$$k_\alpha(power, bdwdth, rate) = \sum_{i=0}^{n}\sum_{j=0}^{n-i} k_\alpha coeff_{ij}(power)\, bandwidth\ \times repetition\ rate$$

$$\delta(power, bdwdth, rate) = \sum_{i=0}^{n}\sum_{j=0}^{n-i} \delta coeff_{ij}(power)\, bandwidth\ \times repetition\ rate$$

Figure 4. Steps involved in modeling process

A. Data Preparation

The first step requires the creation of interference scenarios with diverse chirp signal characteristics. Signal attributes including power, bandwidth and repetition rate are changed within a realistic range. We considered 50 values of sweep rate between [10 – 100 us], 75 values of bandwidth from [1 – 12 MHz] and 15 power levels changing JSR between [5 – 40 dB] to simulate the proximity of the jamming source. The complete procedure involved in the creation of the database is shown in figure 4. In each iteration, a new interfered scenario is recorded after combining pre-recorded GNSS and interference signals with a 15MHz sampling rate. Thanks to Stella IQ record and playback system provided by M3systems we created a database with more than fifty thousand scenarios.

B. Labeling database

The labeling process provides meaningful tags or labels to the input. Here, the objective is to link the optimal combination of pole contraction factor and adaptation step of the ANF to each scenario. An extensive search has been made in pursuit of an optimal combination. A root mean square error (RMSE) criterion is chosen to find the best compromise to recover the GNSS signal after filtering. The RMSE between the reference signal and the filtered signal at the output of the notch filter is computed as:

$$RMSE = \sqrt{\frac{1}{N}\sum_{n=1}^{N}(|x - \hat{x}|)^2}$$

where x is the reference GNSS signal, $\hat{x}$ is the recovered signal after applying the mitigation process and N are the number of observation samples. The existence of one optimal combination drives the search strategy where ANF provides the best performance in terms of retrieval of the GNSS signal. Figure 5 shows the parameter search grid of two interference scenarios with adaptation step and the pole contraction factor is in the x-axis and y-axis while rmse is in the z-axis.

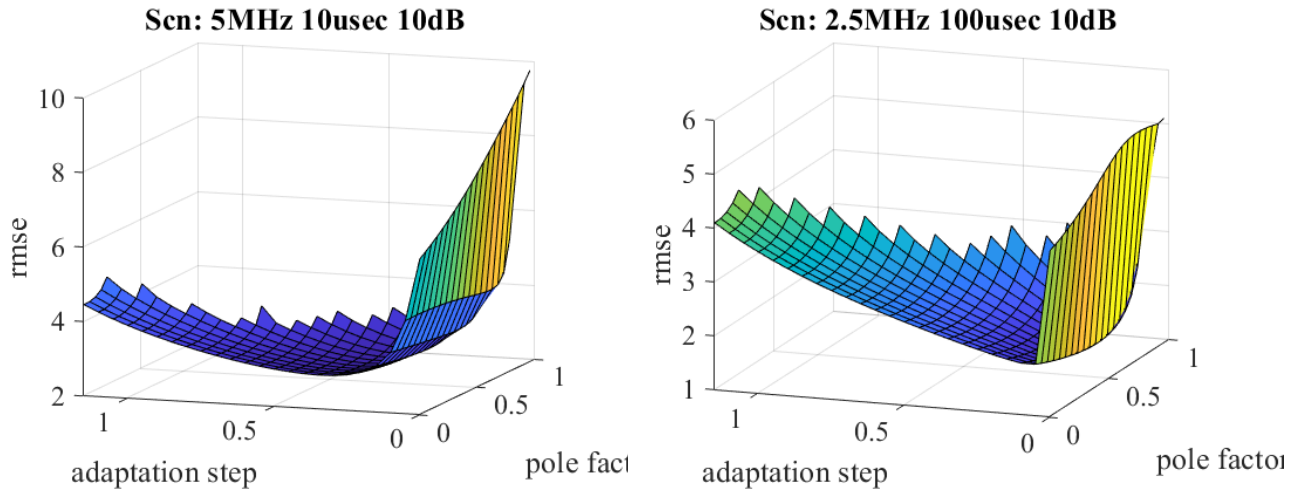

Figure 5. RMSE curves with optimal combination.

The two curves show evidence of a clear region of depression where the RMSE can be found to be relatively minimal. Moreover, the point of minimum shifts for the two cases with a different sweep rate, bandwidth and repetition rate. The parameter combination with the lowest RMSE value is selected as the optimal choice for ANF with the chosen criterion.

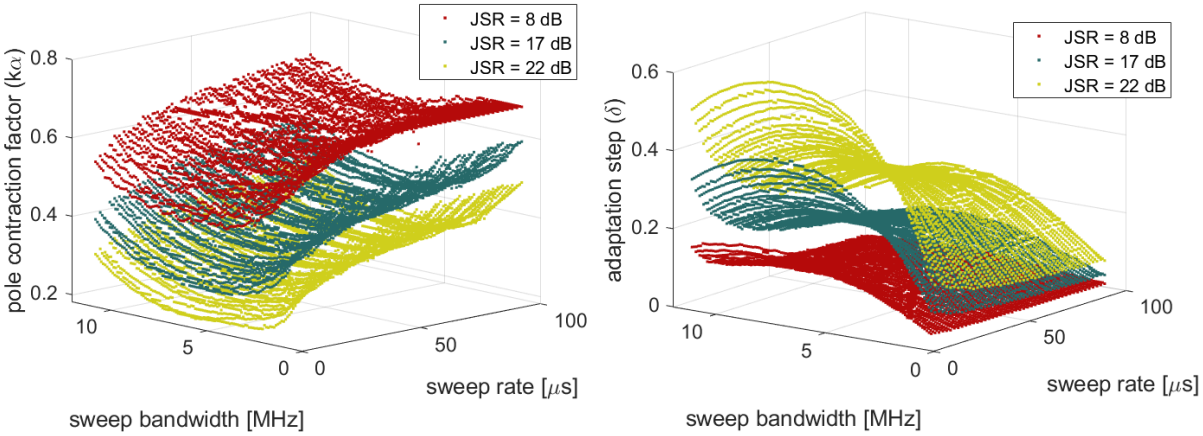

Figure 6. Optimal values of pole factor and adaptation step (measurements) for different chirp scenarios with changing bandwidth and sweep rate for three power level

In the same manner, each of the scenarios of the database is tagged with the optimal output combination (pole factor and adaptation step). Figure 6 shows the selected values of the pole contraction factor and adaptation step representing the minimum value of RMSE for each scenario.

C. MULTIVARIATE POLYNOMIAL REGRESSION (MPR)

Regression analysis is an important statistical method to understand the relationship between two or more variables. Polynomial regression is an extension of linear regression with some additional polynomial terms to describe the nonlinear relationship between the input and the output variable. In general, y estimated from nth-order polynomials yielding a regression model

$$y = p_0 + p_1 x + p_2 x^2 + \cdots + p_n x^n$$

where x is the input variable, y is the output variable and p_n is the coefficient of the nth-order term. A polynomial regression applied to two or more regressor variables is known as Multivariate Polynomial Regression (MPR). A second-order MPR with two variables x_1 and x_2 can be expressed as:

$$y = p_{00} + p_{10} x_1 + p_{01} x_2 + p_{20} x_1^2 + p_{02} x_2^2 + p_{11} x_1 x_2$$

The MPR can be written in a simplified form as:

$$y = \sum_{i=0}^{n} \sum_{j=0}^{n-i} p_{ij}\, x_1 x_2$$

Figure 6 shows a clear pattern depicting some relationship between the input signal features (sweep bandwidth, sweep rate and power) and the selected values of the pole contraction factor k_α and adaptation step δ. Here, the power level appears to shift the curve upward or downward. A two-level regression approach to model the parameters is shown in Figure 7.

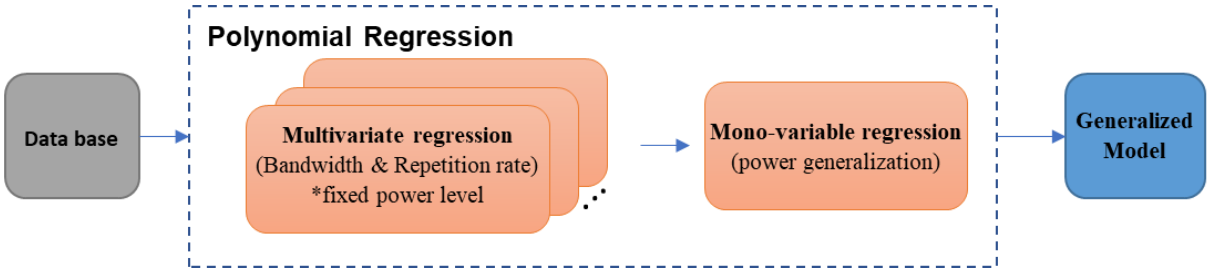

Figure 7. Two-level Regression approach for modelling optimal ANF parameters

In the first level, a multivariate third-order polynomial regression is applied to model the variations of the adaptation step and the pole contraction factor considering the bandwidth and sweep rate as the two input variables with a constant power level. A third order provides a suitable approximation avoiding both overfitting and underfitting of the data points. Figure 8 illustrates the regression curve for the adaptation step and the pole contraction factor approximating variations in the sweep bandwidth and sweep rate for a constant power level of 22 dB JSR.

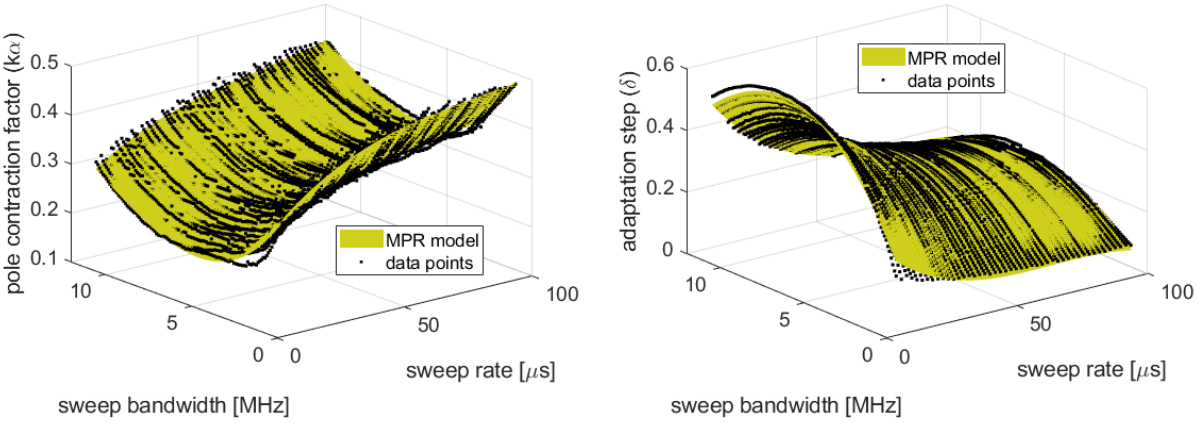

Figure 8. Multivariate regression model for different bandwidth and sweep rate with constant power level (JSR = 22dB)

After performing a regression on individual power levels, a second third-order regression is applied to the approximated coefficients to generalize the power variations. Figure 9 presents an p_{00}, p_{10} and p_{01} coefficients after the regression. In this manner, generalized regression models for 2 output variables (adaptation step and pole contraction factor) are approximated with three input features (sweep rate, bandwidth and power). Considering this new model, figure 10 shows the approximated regression curves generated from complete grid points involving sweep bandwidth and sweep rate for three different power levels. Now from the generalized regression model, predictions are made for three different scenarios to get the optimal choice of parameters. The predicted parameter combination is used to initialize ANF and to perform mitigation. This is detailed in the next section.

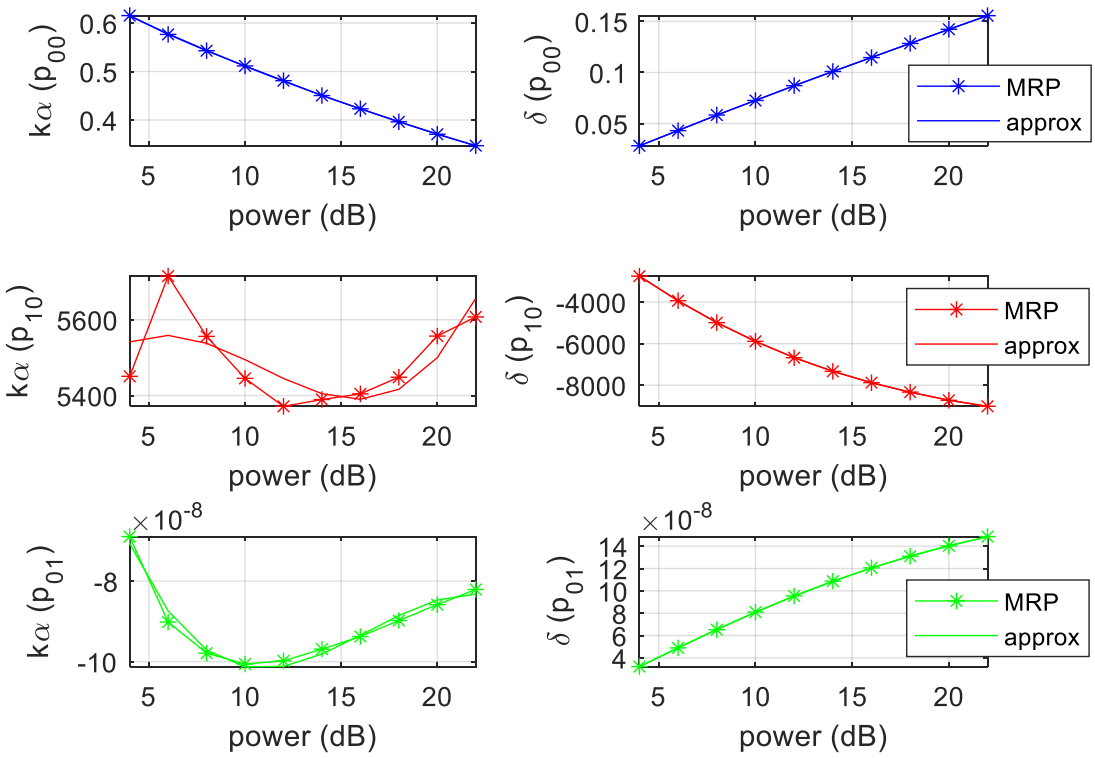

Figure 9. P00, P10 and P01 coefficients of pole factor and adaptation step approximated from the MRP coefficients to generalize power levels in the regression model.

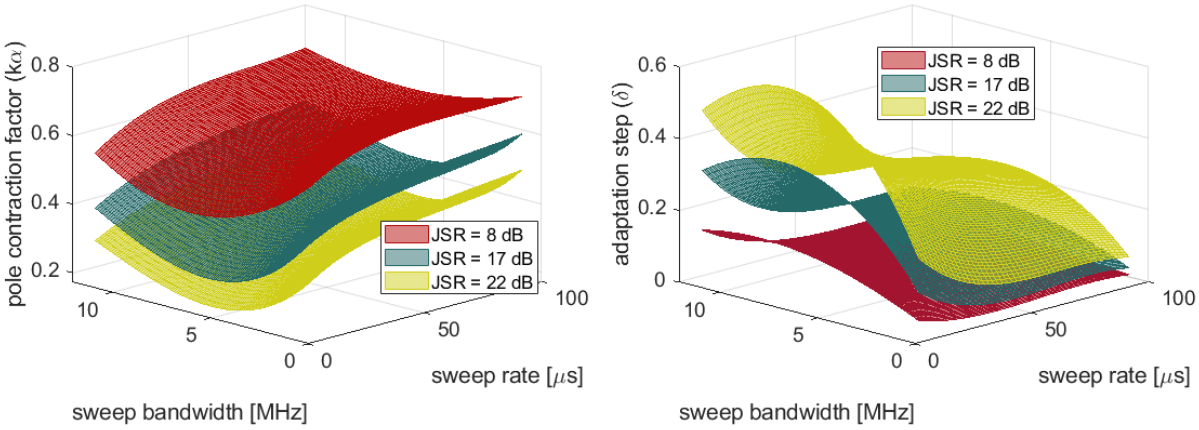

Figure 10. Adaptation step and pole contraction factor curves approximated form the generalized regression model for different values of sweep bandwidth and sweep rate for 3 different power levels.

III. IMPLEMENTATION, RESULTS & ANALYSIS

This section aims to provide a detailed analysis comparing the performance of ANF tuned differently using two different combinations of pole contraction factor k_α and adaptation step δ: the predicted values from the previously presented model and an arbitrary choice selected from the interval presented by most of the studies (Borio & Gioia, 2021; Kazim, Marais, et al., 2022). The performance is analyzed at different signal processing levels including frequency estimation, tracking and carrier-to-noise ratio level. Moreover, the key performance indicators KPIs such as accuracy, availability and safety are also discussed to provide a positioning-level view. We used the tool with record and playback functionality previously presented to create the interference scenario. The prerecorded IQs acquired on 8th February 2023 with GPS L1 (1575.42MHz) as a central frequency and 15MHz sampling rate are

played back. A radio signal recorder (NI-USRP 2954R) connected to the roof antenna placed in relatively open sky conditions is used for this purpose., An interference signal of 30 seconds duration is added at around 50 seconds to ensure normal signal tracking at the start and complete IQs are recorded back with the same recording system. Three chirp scenarios with slow, moderated and fast rates with different power levels are prepared. Table 2 provides the list of scenarios with predicted values of ANF parameters. We now denote 'Set A' to indicate the predicted combination and 'Set B' to indicate the arbitrary parameter choice with $\delta = 0.05$ and $k_\alpha = 0.8$.

Table 2. Predicted combination for three chirp scenarios.

Scenario	Category	Linear chirp parameters			ANF parameters	
		Bandwidth [MHz]	Repetition rate [µs]	JSR level [dB]	Predicted Adaptation Step ($\hat{\delta}$)	Predicted Pole contraction factor ($\hat{k}_\alpha$)
#1	Slow	1	90	17	0.03	0.61
#2	Moderate	5	50	9	0.06	0.55
#3	Fast	7.5	10	14	0.26	0.32

We analyze the impact of the parameter choice in the following different levels: estimation of the notch frequency; signal tracking performance and user KPIs.

- Interference frequency estimation

Figure 11 shows the notch frequency estimated by the ANF, providing a performance comparison for tracking the interference signal with Set A and Set B for three different chirp signals. In all the cases, Set A (blue curve) appears to be the optimal choice for ANF. It allows the filter to closely track the interference frequency and also reduce the noise in the frequency estimation. Figure 11c shows that, in scenario 3, ANF tuned with Set B (purple curve) appears to be relatively less reactive to rapid variations in fast chirp signal. It acquired approximated 2µs more time before reconverging to the interference frequency.

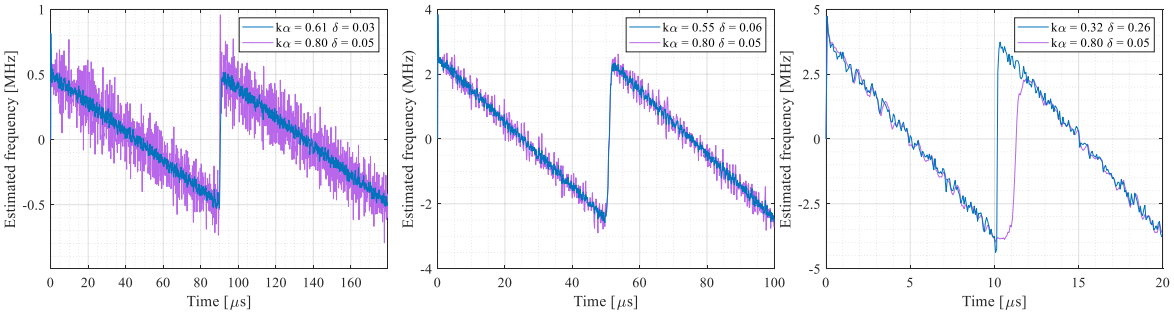

Figure 11. notch frequency estimated by the ANF for the three scenarios with a) slow (Left), b) moderate (middle) and c) fast (right) chirp with predicted (Blue) and fixed (Purple) values of ANF parameters.

- Satellite signal tracking

Figure 12 shows the tracking performance of the satellite (PRN 22) in the three chirp scenarios where the green curve represents the tracking in the nominal conditions. In each case, with the emergence of the interference signal, the tracking loop shows divergence at 50 seconds after losing the lock. At the same time, it starts tracking the interference signal. This seems to unreasonably increase the CN0 level which appears to be at a similar level as in the nominal

conditions as shown in figures 13b and 13c. Scenario 3 with fast chirp appears to be more challenging and shows much more deviation as it accumulated large tracking errors. However, as shown in figures 12a and 13a, applying filtering operation using Set A (blue curve), the tracking loop retrieves back the satellite signal with relatively less tracking noise hence also improving the CN0 estimation in scenario 1. In the same case, Set B (purple curve) displays larger fluctuations during the tracking and also in the CN0 level. In scenario 2, both Set A and Set B show very similar performance in tracking and CN0 level as shown in figure 12b and 13b. In the case of scenario 3 with a fast-varying chirp, surprisingly, Set A appears to be an inadequate choice in finding a reasonable compromise interference removal. As seen previously, a wide notch ($k_\alpha = 0.32$) with large steps ($\delta = 0.26$) appeared to be better in tracking the interference frequency however it is unable to suppress sufficiently the interference content probably due to a wider notch. As a result, it brings relatively more noise in tracking the satellite signal and low CN0 level compared to Set B as shown in figure 12c and 13c.

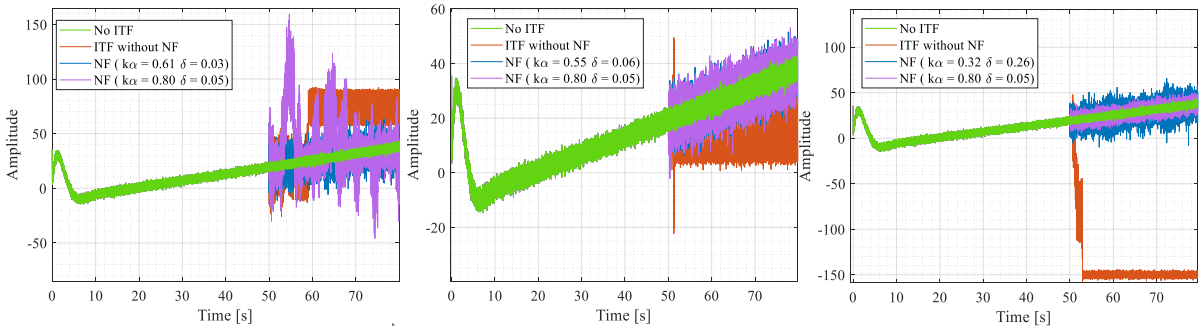

Figure 12. tracking performance (PRN 22) in the three scenarios with a) slow (left), b) moderate (middle) and c) fast (right) chirp; reference - without interference (green), interference without mitigation (red), mitigation with ANF using predicted parameters (blue) and fixed parameters (purple)

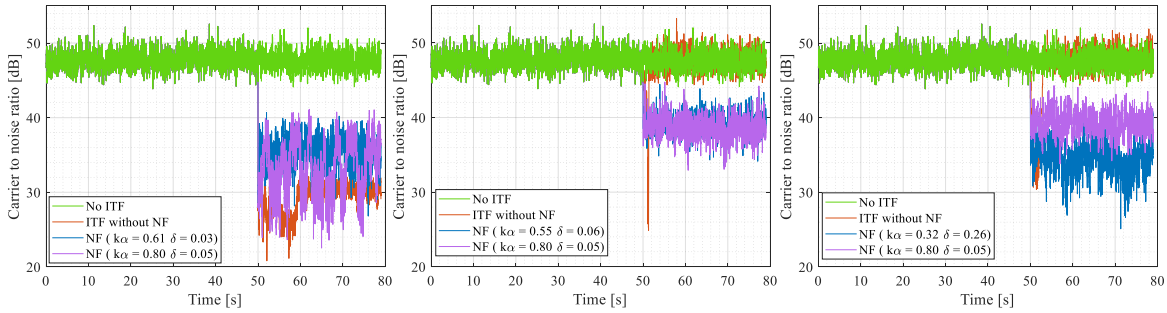

Figure 13. Estimated carrier to noise ratio of satellite (PRN 22) for the three scenarios with a) slow (left), b) moderate (middle) and c) fast (right) chirp; reference - without interference (green), interference without mitigation (red), mitigation with ANF using Set A (blue) and Set B (purple).

- Positioning level

We now analyze results at the position level presenting the impact of interference and the effectiveness of mitigation on KPIs such as accuracy, availability and safety. A Stanford representation is used as it provides a conclusive assessment of the KPI with a simple illustration. The position is estimated using the weighted least square (WLS) algorithm while the hybrid model (product of carrier-to-noise ratio and sine-elevation model) is used to estimate the covariance. Figure 14 shows a Stanford diagram presenting positioning performance in the nominal conditions without the inclusion of interference. It generalizes the maximum achievable performance expected from the same receiver configuration under nominal conditions and is used as a reference for the comparison. In nominal conditions, all the points appear in normal operation (white) with zero unavailable (yellow) and (or)

HMI (red) instances. Figure 15 shows the impact of interference in the three cases with slow, moderate and fast chirp. Here the 62.25% points that appear in the normal operation (white) represent interference-free instances. The remaining 37.5% points represent 30 seconds of interference duration. In all the cases, interference shows an adverse impact on the KPIs. The positioning accuracy is significantly reduced with HPE >50m. Furthermore, the unbounded errors represented by HMI (red) completely expose the positioning system vulnerability and necessitates the mitigation strategy to ensure positioning safety.

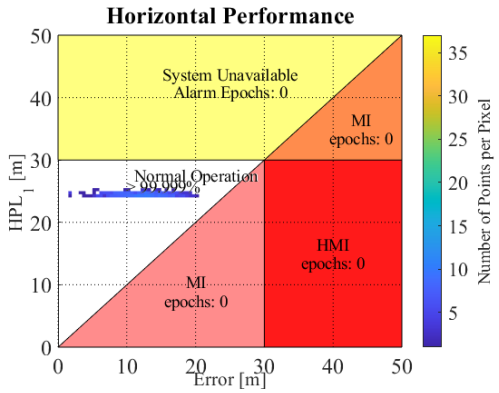

Figure 14. Stanford Diagram Representing Positioning Performance in Nominal Condition

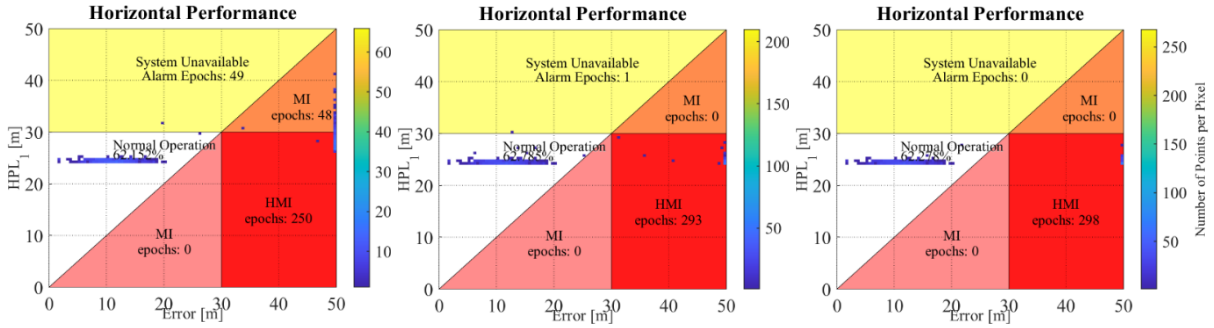

Figure 15. Stanford Diagram Representing Positioning Performance for the three case with a) slow, b) moderate and c) fast chirp before mitigation.

Figure 16 now shows the positioning performance of scenario 1 (bandwidth = 1MHz, repetition rate = 70us and JSR = 17dB) after applying ANF mitigation using Set A and Set B parameters. The ANF mitigation with Set A parameters appears to improve significantly the positioning performance as compared to the Set B combination. It reduces the positioning error (HPE <28m) while increasing normal operation (white) to ~83% with 130 unavailable (yellow) and 1 MI (pink) instances. However, Set B couldn't retrieve the positioning performance at the same level as Set A. It has relatively lower positioning accuracy with many instances having HPE >50m. Additionally, It could not ensure safe positioning entirely with 135 HMI (red), 143 unavailable and 112 MI (pink & orange) instances.

In the case of scenario 2, both parameter combinations Set A and Set B provided very similar performance as shown in Figure 17. Nevertheless, Set A still shows relatively better performance with ~96% of the points in normal operation (white), 30 unavailable points and 0 HMI, while in Set B ~93% of the points appear in normal operation with 49 unavailable, 1 MI and 3 HMI instances.

Figure 18 shows the positioning performance in the third scenario with ANF mitigation using Set A and Set B. In this case, the Set A parameter could not improve as much as in the previous scenarios. It has ~75% normal operation (white) with 127 unavailable (yellow), 50 MI (pink & orange) and 60 HMIs

respectively. However, Set B appears to have performed better with ~95% normal operation (white), 25 unavailable (yellow), 11 MI (pink & orange) and 9 HMI instances.

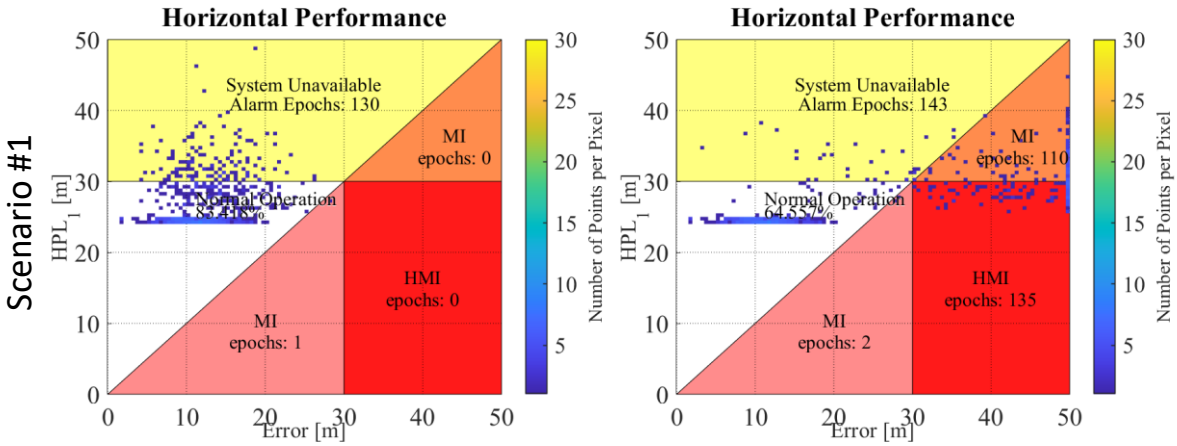

Figure 16. Stanford Diagram Representing Performance after applying mitigation in the first scenario with slow varying chirp (bandwidth = 1MHz, repetition rate = 70us and JSR = 17dB) using ANF a) Set A (δ=0.03 and k_α= 0.61) and b) Set B (δ = 0.05 and k_α=0.8)

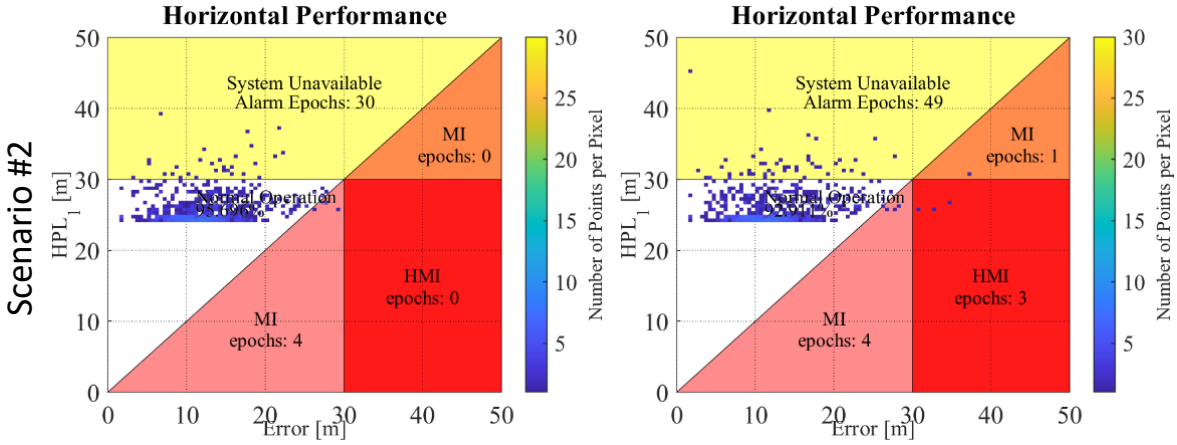

Figure 17. Stanford Diagram Representing Performance after applying mitigation in scenario 2 with moderate chirp (bandwidth = 5MHz, repetition rate = 50us and JSR = 9dB) using ANF a) Set A (δ = 0.06 and k_α= 0.55) and b) Set B (δ = 0.05 and k_α= 0.8)

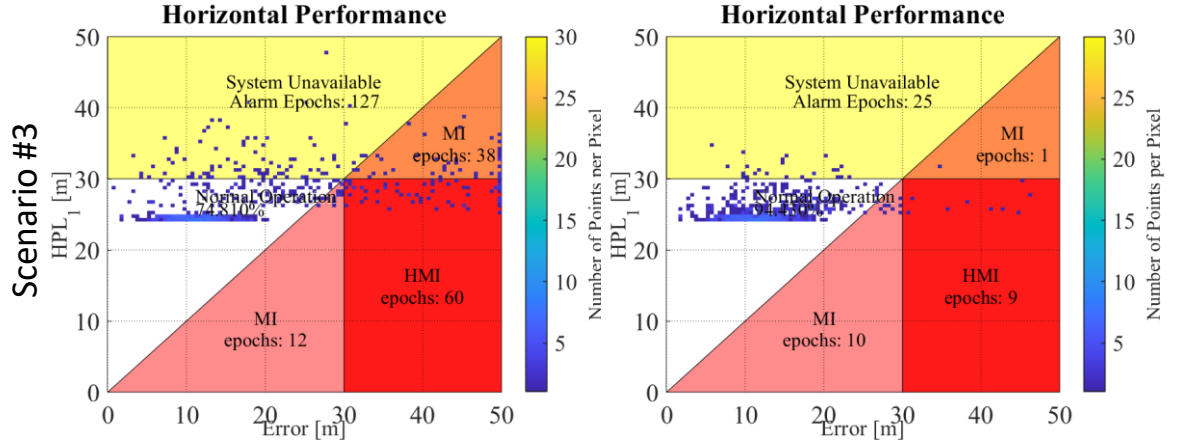

Figure 18. Stanford Diagram Representing Performance after applying mitigation in the third scenario with fast varying chirp (bandwidth = 7.5MHz, repetition rate = 10us and JSR = 14dB) using ANF combination a) Set A (δ = 0.06 and k_α = 0.55) and b) Set B (δ = 0.05 and k_α= 0.8)

Conclusion and discussion

This study validates the initial postulate that an appropriately tuned ANF enhance effectively the suppression of chirp-like interference signal. It also contributes to the retrieval of acceptable performance indicators while dealing with safety concerns depending on the severity of the jammer. In safety-critical applications, positioning availability is not solely defined by the ability to provide the positioning estimate. It also requires that the positioning error is well bounded and remains below the alarm limit. In (Kazim, Marais, et al., 2022), we have seen that ANF is capable of removing the HMI events to ensure safe localization but it is conditioned to the selection of the parameters. However, most of the points were replaced with unavailability (PE<AL<PL). This particularly happens while considering CN0 measurements in the weighting model. The two following complementary actions could allow better availability: 1) an optimal choice of ANF parameters and 2) a specific calibration of the weighting model with probably a less conservative approach after mitigation.

This study is based on the assumption that a rapid and precise characterization of the interference signal is possible and available. The characterization would make it possible to evaluate jammer features including the type of interference signal, perceived band power, bandwidth occupancy and the repetition rate. To study the sensitivity of the optimal parameters choice while considering the characterization error is motivating nevertheless it is considered out of scope for this work.

We presented a simple approach even if it requires quite a large number of simulations to create the models to select the ANF tunable parameters. The predicted parameters for scenario 1 and scenario 2 made it possible to remove all the HMI and also reduce the unavailability compared to the policy of naively fixing the values of pole contraction factor ($k\alpha = 0.8$) and adaptation step ($\delta = 0.05$). However, it completely underperformed for scenario 3 with a fast chirp. A further investigation revealed that RMSE despite covering the complete interference bandwidth could not find much needed compromise in the removal of necessary unwanted content from the signal. On the other hand, naively chosen combination even though took longer time to converge but with the narrow notch still managed to efficiently remove the unwanted content. This probably appear to be a compromise of leaving some interference residue on the far end and to precisely target the interference close to the central frequency which appear to be very effective. A weighting policy in RMSE computation while giving more importance to IQs close to the central frequency could be investigated in the future. The initial results shows that the policy considered to be optimal at the signal level is not necessarily the ideal at the positioning or RAIM level. It also opens possibilities to assess other metrics where the optimal criterion could be applied at position level.

References

Anyaegbu, E., Brodin, G., Cooper, J., Aguado, E., & Boussakta, S. (2008). An integrated pulsed interference mitigation for GNSS receivers. *The Journal of Navigation*, *61*(2), 239.

Borio, D. (2016). Loop analysis of adaptive notch filters. *IET Signal Processing*, *10*(6), 659–669.

Borio, D., Camoriano, L., Savasta, S., & Presti, L. Lo. (2008). Time-Frequency Excision for GNSS Applications. *IEEE Systems Journal*, *2*(1), 27–37. https://doi.org/10.1109/JSYST.2007.914914

Borio, D., & Cano, E. (2013). Optimal global navigation satellite system pulse blanking in the presence of signal quantisation. *IET Signal Processing*, *7*(5), 400–410.

Borio, D., & Gioia, C. (2021). GNSS interference mitigation: A measurement and position domain assessment. *Navigation, Journal of the Institute of Navigation*, *68*(1), 93–114. https://doi.org/10.1002/navi.391

Dey, A., Iyer, K., Sharma, N., & Campus, K. K. B. G. (2021). *S-band Interference Detection and Mitigation using a Vector Tracking-based NavIC Software Receiver*. 3464–3476.

Dovis, F. (2015). *GNSS Interference Threats and Countermeasures*. Artech House.

Dovis, F., Musumeci, L., & Samson, J. (2012). Performance comparison of transformed-domain techniques for pulsed interference mitigation. *Proceedings of the 25th International Technical Meeting of the Satellite Division of The Institute of Navigation (ION GNSS 2012)*, 3530–3541.

Felber, W. (n.d.). *Adaptive notch filtering against complex interference scenarios*. 1–10.

Fu, Z., Hornbostel, A., Hammesfahr, J., & Konovaltsev, A. (2003). Suppression of multipath and jamming signals by digital beamforming for GPS/Galileo applications. *GPS Solutions*, *6*(4), 257–264.

Groves, P. D., & Long, D. C. (2005). Combating GNSS interference with advanced inertial integration. *The Journal of Navigation*, *58*(3), 419.

Gupta, I. J., & Moore, T. D. (2003). Space-frequency adaptive processing (SFAP) for RFI mitigation in spread spectrum receivers. *IEEE Antennas and Propagation Society International Symposium. Digest. Held in Conjunction with: USNC/CNC/URSI North American Radio Sci. Meeting (Cat. No. 03CH37450)*, *4*, 172–175.

Kazim, S. A., Marais, J., & Tmazirte, N. A. (2022). Interferences in Safety Critical Land Transport Application: Notch Filtering vs Wavelet Transform, an Experimental Analysis. *Proceedings of the 35th International Technical Meeting of the Satellite Division of The Institute of Navigation (ION GNSS+ 2022)*, 3743–3757. https://doi.org/10.33012/2022.18563

Kazim, S. A., Tmazirte, N. A., Marais, J., & Tsaturyan, A. (2022). On the impact of jamming on Horizontal Protection Level and Integrity Assessment for Terrestrial Localization. *Proceedings of the International Technical Meeting of The Institute of Navigation, ITM*, *2022-Janua*, 1343–1357. https://doi.org/10.33012/2022.18223

Kraus, T., Bauemfeind, R., & Eissfeller, B. (2011). Survey of In-Car Jammers - Analysis and modeling of the RF signals and IF samples (suitable for active signal cancellation). *24th International Technical Meeting of the Satellite Division of the Institute of Navigation 2011, ION GNSS 2011*, *1*.

Musumeci, L., & Dovis, F. (2014). Use of the wavelet transform for interference detection and mitigation in global navigation satellite systems. *International Journal of Navigation and Observation*, *2014*. https://doi.org/10.1155/2014/262186

Qin, W., Gamba, M. T., Falletti, E., & Dovis, F. (2019). Effects of Optimized Mitigation Techniques for Swept-frequency Jammers on Tracking Loops. *Proceedings of the 32nd International Technical Meeting of the Satellite Division of the Institute of Navigation, ION GNSS+ 2019*, 3275–3284. https://doi.org/10.33012/2019.17067

Qin, W., Gamba, M. T., Falletti, E., & Dovis, F. (2020). An Assessment of Impact of Adaptive Notch Filters for Interference Removal on the Signal Processing Stages of a GNSS Receiver. *IEEE Transactions on Aerospace and Electronic Systems*, *56*(5), 4067–4082. https://doi.org/10.1109/TAES.2020.2990148

Stallo, C., Salvatori, P., Coluccia, A., Neri, A., & Rispoli, F. (2020). GNSS anti-JAM RF-to-RF on board unit for ERTMS train control. *ION 2020 International Technical Meeting Proceedings*, 1045–1058. https://doi.org/10.33012/2020.17196

Szumski, A., & Eissfeller, B. (2013). The Karhunen-Loeve transform as a future instrument to interference mitigation. *Proceedings of the 26th International Technical Meeting of the Satellite Division of The Institute of Navigation (ION GNSS+ 2013)*, 3443–3449.